

Binuclear Homoleptic Copper Carbonyls $\text{Cu}_2(\text{CO})_x$ ($x = 1-6$): Remarkable Structures Contrasting Metal–Metal Multiple Bonding with Low-Dimensional Copper Bonding Manifolds

Qianshu Li and Yongdong Liu

School of Chemical Engineering and Materials Science, Beijing Institute of Technology, Beijing, China 100081

Yaoming Xie, R. Bruce King, and Henry F. Schaefer III*

Center for Computational Quantum Chemistry, University of Georgia, Athens, Georgia 30602-2556

Received July 20, 2001

Binuclear homoleptic copper carbonyls $\text{Cu}_2(\text{CO})_x$ ($x = 1-6$) have been studied using four different density functional theory methods (DFT) in conjunction with a basis set of extended double- ζ plus polarization quality, labeled as DZP. For each homoleptic binuclear copper carbonyl compound, several stationary point structures are presented, and these structures are characterized in terms of their geometries, thermochemistry, and vibrational frequencies. The optimal unsaturated $\text{Cu}_2(\text{CO})_x$ ($x = 1-6$) structures are generated by joining 18-electron tetrahedral, 16-electron trigonal, 14-electron linear copper carbonyl building blocks, and/or bare copper atoms with copper–copper single bonds rather than by joining 18-electron copper carbonyl units with multiple copper–copper bonds. For $\text{Cu}_2(\text{CO})_6$ the eclipsed and staggered ethane-like structure are virtually degenerate and lie significantly lower in energy than other possible structures. The eclipsed Cu–Cu single bond distance is predicted to be 2.61 Å, while that for the staggered structure is 2.65 Å. The lowest energy structure for $\text{Cu}_2(\text{CO})_5$ is the eclipsed ethyl radical-like structure, with $r_e(\text{Cu}-\text{Cu}) = 2.51$ Å. The staggered ethyl radical-like structure lies only 0.1 kcal/mol higher in energy, with a Cu–Cu distance shorter by only ~ 0.001 Å. For $\text{Cu}_2(\text{CO})_4$ a methylcarbene-like structure is predicted to lie lowest, with Cu–Cu distance 2.40 Å. However, twisted and planar ethylene-like structure lie only 3–5 kcal/mol higher. For $\text{Cu}_2(\text{CO})_3$ a surprising methylcarbyne-like structure with $r_e(\text{Cu}-\text{Cu}) = 2.38$ Å is predicted to lie lowest with all four DFT methods. However, a classical vinyl radical-like lies only 2–4 kcal/mol higher. For $\text{Cu}_2(\text{CO})_2$ theory predicts a vinylidene-like structure with $r_e(\text{Cu}-\text{Cu}) = 2.34$ Å to be essentially degenerate with cis and trans bent acetylene structures with copper–copper distances 2.33 Å. Finally, and consistent with earlier theoretical studies, the linear end on Cu–Cu–CO structure with $r_e(\text{Cu}-\text{Cu}) = 2.27$ Å is the predicted global minimum for $\text{Cu}_2(\text{CO})$.

Introduction

Homoleptic transition metal carbonyls are fundamental constituents of modern organometallic chemistry.¹ Binuclear metal carbonyl compounds comprise an important part of the vast class of transition-metal carbonyl complexes.² The $\text{M}_2(\text{CO})_x$ systems are the simplest representatives of transition-metal molecular clusters, which have been studied extensively because of their role in organometallic chemistry and catalysis. Quite a number of studies, experimental and theoretical, have dealt with binuclear complexes of transition metals. Such compounds as $\text{Mn}_2(\text{CO})_{10}$, $\text{Fe}_2(\text{CO})_9$, and $\text{Co}_2(\text{CO})_8$ have been well characterized experimentally.³ Several theoretical studies have been devoted to these compounds^{4–16} with the objective of understanding the observed structural types. According to the simple

18-electron rule, copper should form a saturated binuclear carbonyl with the formula $\text{Cu}_2(\text{CO})_6$.

The early literature contains many scattered claims for the existence of binary copper carbonyls.^{17–19} In 1975 Huber, Kündig, Moskovits, and Ozin²⁰ were able to obtain impressive evidence for $\text{Cu}(\text{CO})_3$, $\text{Cu}(\text{CO})_2$, $\text{Cu}(\text{CO})$, and $\text{Cu}_2(\text{CO})_6$ using

- (1) Cotton, F. A.; Wilkinson, G.; Murillo, C. A.; Bochmann, M. *Advanced Inorganic Chemistry*, 6th ed.; John Wiley: New York, 1999.
- (2) Calderazzo, F. In *Encyclopedia of Inorganic Chemistry*; King, R. B., Ed.; Wiley: Chichester, 1994; pp 560–575.
- (3) Cotton, F. A.; Troup, J. M. *J. Chem. Soc., Dalton Trans.* **1974**, 800.
- (4) Cotton, F. A. *Prog. Inorg. Chem.* **1976**, 21, 1.
- (5) Fenske, R. F. *Prog. Inorg. Chem.* **1976**, 21, 179.
- (6) Klinger, R. J.; Butler, W. M.; Curtis, M. D. *J. Am. Chem. Soc.* **1978**, 100, 5034.

- (7) Jemmis, E. D.; Pinhas, A. R.; Hoffmann, R. *J. Am. Chem. Soc.* **1980**, 102, 2576.
- (8) Lauher, J. W.; Elian, M.; Summerville, R. H.; Hoffmann, R. *J. Am. Chem. Soc.* **1976**, 98, 3219.
- (9) Sargent, A. L.; Hall, M. B. *J. Am. Chem. Soc.* **1989**, 111, 1563.
- (10) Simpson, C. Q.; Hall, M. B. *J. Am. Chem. Soc.* **1992**, 114, 1641.
- (11) Folga, E.; Ziegler, T. *J. Am. Chem. Soc.* **1993**, 115, 5169.
- (12) Ziegler, T. *Can. J. Chem.* **1995**, 73, 743.
- (13) Jang, J. H.; Lee, J. G.; Lee, H.; Xie, Y.; Schaefer, H. F. *J. Phys. Chem. A* **1998**, 102, 5298.
- (14) Ignatyev, I. S.; Schaefer, H. F.; King, R. B.; Brown, S. T. *J. Am. Chem. Soc.* **2000**, 122, 1989.
- (15) Xie, Y.; Schaefer, H. F.; King, R. B. *J. Am. Chem. Soc.* **2000**, 122, 8746.
- (16) Kenny, J.; King, R. B.; Schaefer, H. F. *Inorg. Chem.* **2001**, 40, 900.
- (17) Kunz-Krause, H. *Apoth. Ztg.* **1916**, 31, 66.
- (18) Plotnikov, V. A.; Ivanov, K. N. *Zh. Khim. Promsti.* **1930**, 7, 1136.
- (19) Pospekhov, D. A. *Zh. Prikl. Khim.* **1946**, 19, 848.
- (20) Huber, H.; Kündig, E. P.; Moskovits, M.; Ozin, G. A. *J. Am. Chem. Soc.* **1975**, 97, 2097.

the co-condensation reaction of copper atoms with carbon monoxide in conjunction with matrix isolation infrared and UV-vis spectroscopy. Subsequently Kasai and Jones²¹ observed $\text{Cu}(\text{CO})_3$ and $\text{Cu}_2(\text{CO})_6$ at much lower temperatures. Howard, Mile and their co-workers^{22–26} also unequivocally confirmed that the deposits, which were red-purple, consisted of the copper carbonyls $\text{Cu}(\text{CO})_3$ and $\text{Cu}_2(\text{CO})_6$. They also performed a more thorough spectroscopic study on the carbonyls produced from Cu and CO in inert hydrocarbon matrixes at 77 K in a rotating cryostat. Later they also used the rotating cryostat technique to produce the copper carbonyls $\text{Cu}_n(\text{CO})_m$, $n = 1–2$, $m = 1–6$, in adamantane.

The aim of the present research was to predict plausible structures, vibrational frequencies, and energetics for the homoleptic binuclear copper carbonyl compounds, and to attempt to explain these results in terms of simple models.

Theoretical Methods

Electron correlation effects were included employing DFT methods, which have been recognized as a practical and effective computational tool, especially for organometallic compounds.¹² Four different density functional or hybrid Hartree-Fock/Density functional forms were used in our studies. The first, designated B3LYP, is an HF/DFT hybrid method implemented in the Gaussian program.²⁷ The B3LYP method (also an HF/DFT hybrid method) is formed from Becke's three-parameter semiempirical exchange functional (B3)²⁸ along with the Lee, Yang and Parr correlation functional (LYP).²⁹ The BP86 method uses Becke's 1988 exchange functional (B)³⁰ with the Perdew correlation functional (P86).³¹ Finally, the BLYP method merges the Becke (B) exchange functional with the LYP correlation functional.

The basis sets for C and O begin with Dunning's standard double- ζ (DZ) contraction³² of Huzinaga's primitive sets³³ and are designated as (9s5p/4s2p). The double- ζ plus polarization (DZP) basis sets used here add one set of pure spherical harmonic d functions with orbital exponents $\alpha_d(\text{C}) = 0.75$ and $\alpha_d(\text{O}) = 0.85$ to the DZ basis set. For Cu, in our DZP basis set, the Wachter's primitive sets³⁴ is loosely contracted, but augmented by two sets of p functions and one set of d functions, contracted following Hood et al.,³⁵ and designated as (14s11p6d/10s8p3d).

We fully optimized the geometries of all structures using analytic first derivatives of the energy with respect to the nuclear coordinates. We also determined the harmonic vibrational frequencies associated with each stationary point by evaluating analytically the second derivatives of the energy with respect to the nuclear coordinates. The computations were carried out with the Gaussian 94 program,³⁶ in which the fine grid (75,302) is the default for evaluating integrals numerically, and the tight (10^{-8} hartree) designation is the default for the self-

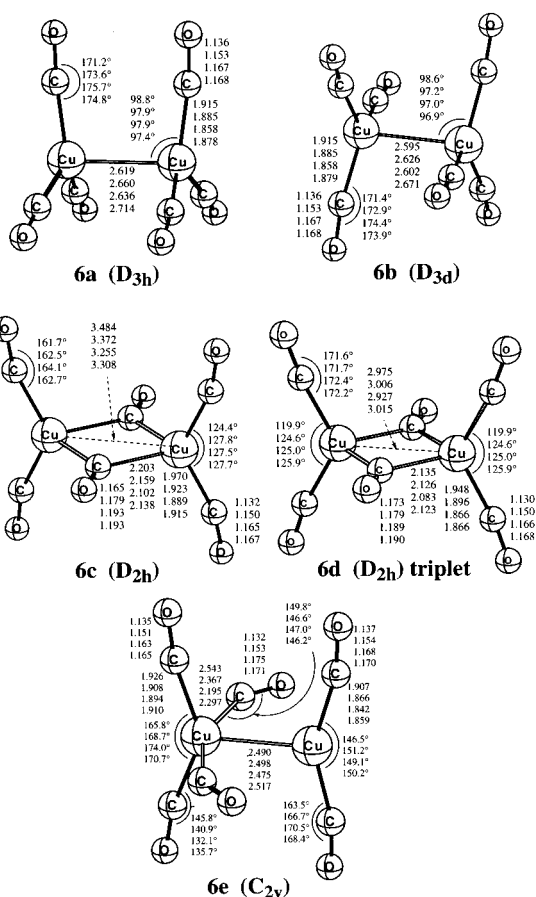


Figure 1. Structures of $\text{Cu}_2(\text{CO})_6$, with bond distances in Å.

consistent field (SCF) convergence. The predicted structures are depicted in Figures 1–6 with all bond distances given in Å.

Relativity seems to play a minor role in structural predictions for most systems incorporating first-row transition metals. However, some exceptions for copper systems have been reported. For example, Antes and Frenking³⁷ discuss this problem in their work on the $\text{Cu}-\text{CH}_3$ system. However, at this early stage in the investigation of such a broad range of copper carbonyls, we neglect relativistic effects.

Results

A. Molecular Structures. I. $\text{Cu}_2(\text{CO})_6$. Five $\text{Cu}_2(\text{CO})_6$ structures are obtained in this research, and they are shown in Figure 1. The structures **6a** and **6b** present the unbridged D_{3h} and D_{3d} ethane-like structures of $\text{Cu}_2(\text{CO})_6$. These structures both have the lowest energies with all four DFT methods (see Table 1). The eclipsed D_{3h} structure **6a** lies 0.43 kcal/mol (B3LYP) or 0.09 kcal/mol (B3LYP) lower than the staggered D_{3d} structure **6b**, but it is higher by 0.27 and 0.15 kcal/mol with the BP86 and BLYP methods. Structure **6b** is a genuine minimum. Structure **6a** is predicted as a minimum using the B3LYP and BLYP methods, but has a small imaginary frequency, which leads to **6b**, using the BP86 and BLYP methods. The Cu–Cu distance (in Figure 1) for the eclipsed

- (21) Kasai, P. H.; Jones, P. M. *J. Am. Chem. Soc.* **1985**, *107*, 813.
 (22) Howard, J. A.; Mile, B.; Morton, J. R.; Preston, K. F.; Sutcliffe, R. *Chem. Phys. Lett.* **1985**, *117*, 115.
 (23) Howard, J. A.; Mile, B.; Morton, J. R.; Preston, K. F. *J. Phys. Chem.* **1986**, *90*, 1033.
 (24) Howard, J. A.; Mile, B.; Morton, J. R.; Preston, K. F. *J. Phys. Chem.* **1986**, *90*, 2027.
 (25) Chenier, J. H. B.; Hampson, C. A.; Howard, J. A.; Mile, B. *J. Phys. Chem.* **1989**, *93*, 114.
 (26) Mile, B.; Howard, J. A.; Tomietto, M.; Joly, H. A.; Sayari, A. *J. Mater. Sci.* **1996**, *31*, 3073.
 (27) The functional employed by keyword BHandHLYP to Gaussian94 is: $0.5*\text{Ex}(\text{LSDA}) + 0.5*\text{Ex}(\text{HF}) + 0.5*\text{Delta-Ex}(\text{B88}) + \text{Ec}(\text{LYP})$. Note that this is not the formulation proposed by Becke in his 1993 paper.
 (28) Becke, A. D. *J. Chem. Phys.* **1993**, *98*, 5648.
 (29) Lee, C.; Yang, W.; Parr, R. G. *Phys. Rev. B* **1988**, *37*, 78.
 (30) Becke, A. D. *Phys. Rev. A* **1988**, *38*, 3098.
 (31) Perdew, J. P. *Phys. Rev. B* **1986**, *33*, 8822; *34*, 7046.
 (32) Dunning, T. H. *J. Chem. Phys.* **1970**, *53*, 2823.
 (33) Huzinaga, S. *J. Chem. Phys.* **1965**, *42*, 1293.
 (34) Wachters, A. J. H. *J. Chem. Phys.* **1970**, *52*, 1033.
 (35) Hood, D. M.; Pitzer, R. M.; Schaefer, H. F. *J. Chem. Phys.* **1979**, *71*, 705.

- (36) Frisch, M. J.; Trucks, G. W.; Schlegel, H. B.; Gill, P. M. W.; Johnson, B. G.; Robb, M. A.; Cheeseman, J. R.; Keith, T.; Petersson, G. A.; Montgomery, J. A.; Raghavachari, K.; Al-Laham, M. A.; Zakrzewski, V. G.; Ortiz, J. V.; Foresman, J. B.; Cioslowski, J.; Stefanov, B. B.; Nanayakkara, A.; Challacombe, M.; Peng, C. Y.; Ayala, P. Y.; Chen, W.; Wong, M. W.; Andres, J. L.; Replogle, E. S.; Gomperts, R.; Martin, R. L.; Fox, D. J.; Binkley, J. S.; Defrees, D. J.; Baker, J.; Stewart, J. P.; Head-Gordon, M.; Gonzalez, C.; Pople, J. A. *Gaussian 94*, revision B.3; Gaussian, Inc.: Pittsburgh, PA, 1995.
 (37) Antes, I.; Frenking, G. *Organometallics* **1995**, *14*, 4263.

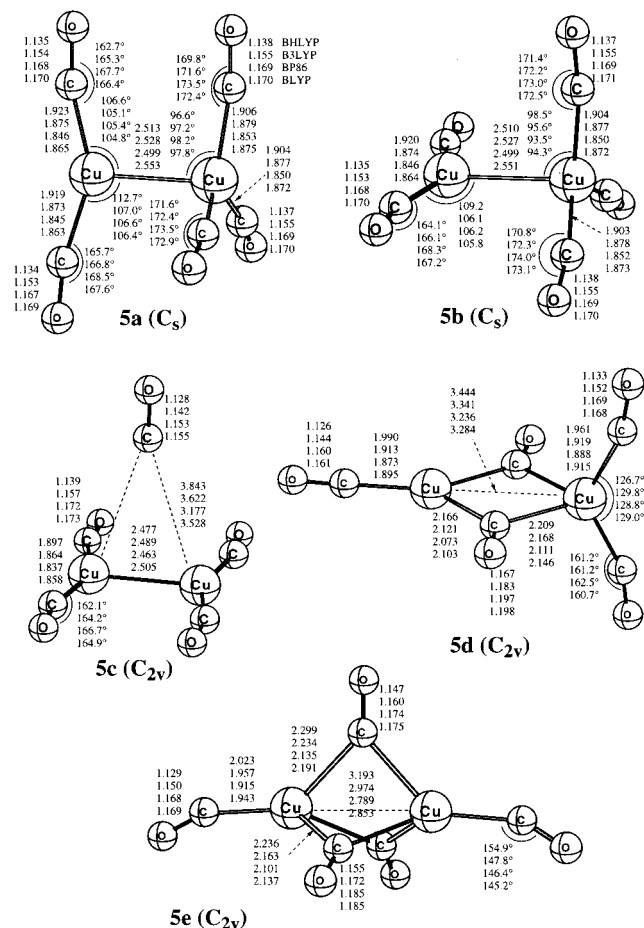


Figure 2. Structures of $\text{Cu}_2(\text{CO})_5$, with bond distances in Å.

D_{3h} structure (2.619 Å BHLYP, 2.660 Å B3LYP, 2.636 Å BP86, and 2.714 Å BLYP) is predicted to be slightly longer (by 0.02, 0.03, 0.03, and 0.04 Å, respectively) than that for the staggered D_{3d} structure. To satisfy the 18-electron rule, these structures must incorporate a Cu–Cu single bond. Note that the copper–copper distances of both the unbridged structures are close to the sum of two copper atom radii (1.28 Å). Furthermore, the unbridged structures are consistent with the experimental results obtained by Huber,²⁰ from which $\text{Cu}_2(\text{CO})_6$ was viewed as a dimer derived from two $\text{Cu}(\text{CO})_3$ residues with a Cu–Cu single bond formed by overlap of the highest singly occupied orbital of the $\text{Cu}(\text{CO})_3$ fragment. Our previous theoretical studies^{13,16} of $\text{Fe}_2(\text{CO})_9$ and $\text{Co}_2(\text{CO})_8$ have yielded comparisons with experiment suggesting that the B3LYP and BP86 methods are comparably reliable for structural predictions. Therefore, we obtain our best estimates of the structures predicted herein by averaging the B3LYP and BP86 geometrical parameters. Thus the estimated Cu–Cu single bond distances for the eclipsed and staggered ethane-like structures of $\text{Cu}_2(\text{CO})_6$ are 2.64 and 2.61 Å, respectively.

The $\text{Cu}_2(\text{CO})_6$ dibridged structure **6c** with D_{2h} symmetry is also a genuine minimum, and is shown in Figure 1. The copper–copper distance computed for **6c**, namely, 3.484 Å (BHLYP), 3.372 Å (B3LYP), 3.255 Å (BP86), or 3.308 Å (BLYP), is much longer than that in the above ethane-like structures **6a** and **6b**. In addition there is a significant elevation in energy for the dibridged structure **6c** compared to the unbridged structures. The lowest triplet state for the similar dibridged structure, namely **6d**, is also a genuine minimum and has a lower energy than the singlet structure **6c** by 4–15 kcal/mol, depending on

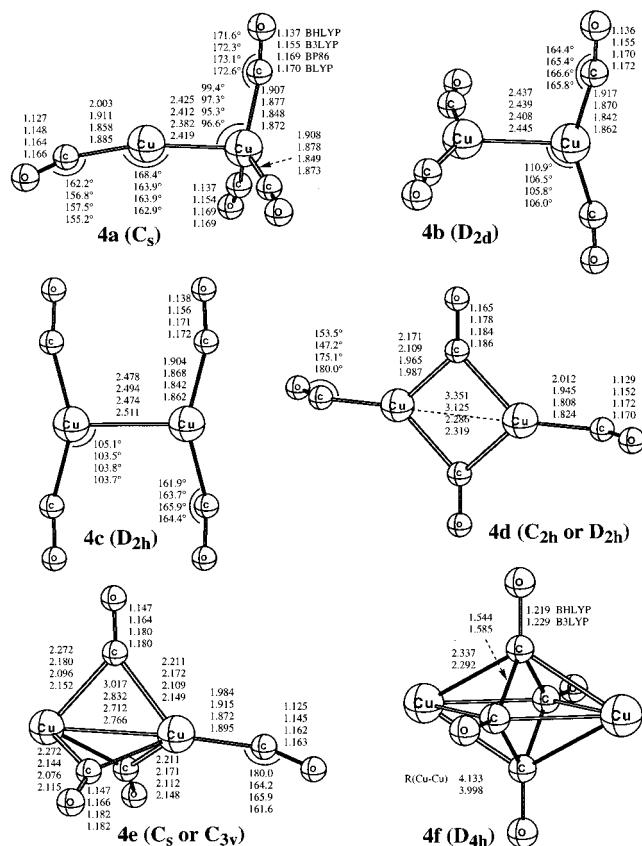


Figure 3. Structures of $\text{Cu}_2(\text{CO})_4$, with bond distances in Å.

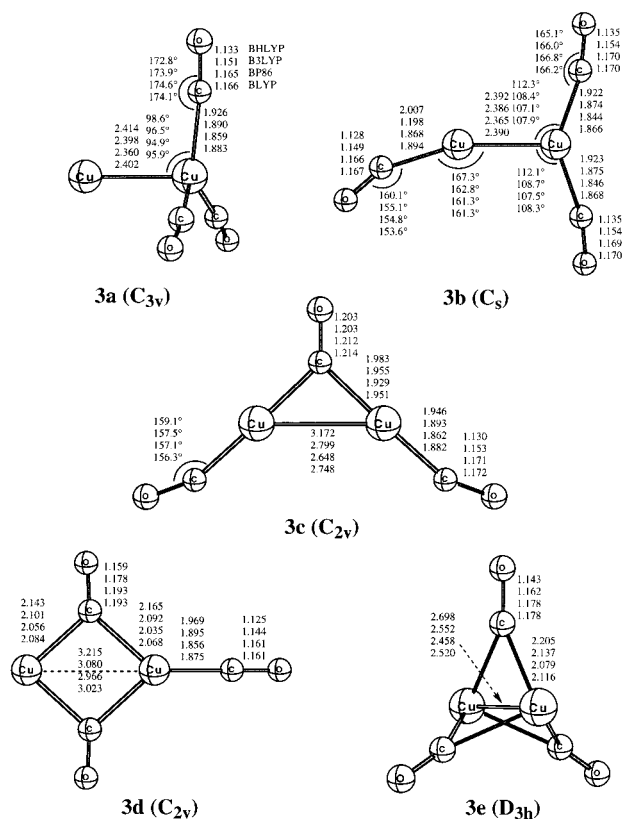


Figure 4. Structures of $\text{Cu}_2(\text{CO})_3$, with bond distances in Å.

the computational method (Table 1). The Cu–Cu distance for triplet **6d** is shorter by about 0.3–0.5 Å than that in structure **6c**, and it is predicted to be 2.975, 3.006, 2.927, 3.015 Å, respectively. The $(\text{CO})_4\text{Cu}-\text{Cu}(\text{CO})_2$ structure **6e** shows a

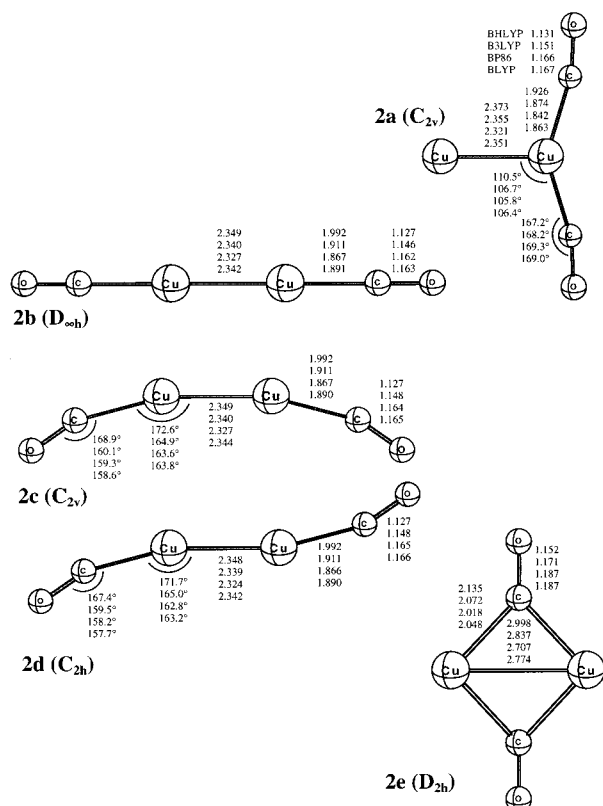


Figure 5. Structures of $\text{Cu}_2(\text{CO})_2$, with bond distances in Å.

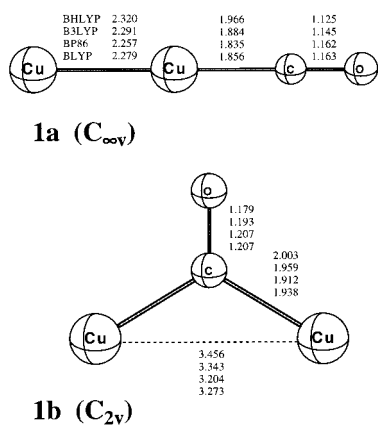


Figure 6. Structures of $\text{Cu}_2(\text{CO})$, with bond distances in Å.

Table 1. The Relative Energies of the $\text{Cu}_2(\text{CO})_6$ Structures, in kcal/mol

		BHLYP	B3LYP	BP86	BLYP
eclipsed ethane-like	6a	0.0	0.0	0.0	0.0
staggered ethane-like	6b	0.4	0.1	-0.3	-0.2
dibridged singlet	6c	38.5	33.7	30.2	29.0
dibridged triplet	6d	23.3	26.4	24.9	25.4
$(\text{CO})_4\text{Cu}-\text{Cu}(\text{CO})_2$	6e	22.3	28.8	34.9	31.8

geometry with C_{2v} symmetry. The Cu—Cu bond distance in **6e** is 2.490 Å (BHLYP), 2.498 Å (B3LYP), 2.475 Å (BP86), or 2.517 Å (BLYP), which is obviously shorter by about 0.9 Å than that for structure **6c**, and shorter by nearly 0.1–0.2 Å than those for the unbridged structures **6a** and **6b**. Table 1 shows that this C_{2v} structure lies 14.5 kcal/mol (BHLYP) and 4.9 kcal/mol (B3LYP) lower than the dibridged D_{2h} structure **6c**; but it is higher by 4.6 and 2.8 kcal/mol with BP86 and BLYP methods. Note, however, that this structure has imaginary vibrational frequencies.

Table 2. The Relative Energies of the $\text{Cu}_2(\text{CO})_5$ Structures, in kcal/mol

		BHLYP	B3LYP	BP86	BLYP
eclipsed ethyl radical-like	5a	0.0	0.0	0.0	0.0
staggered ethyl radical-like	5b	0.2	0.1	0.1	0.1
$\text{CO}\cdots\text{Cu}_2(\text{CO})_4$	5c	15.1	19.1	26.0	21.6
dibridged	5d	33.7	30.5	28.3	27.1
tribridged	5e	34.0	31.6	26.7	27.2

We attempted to optimize a triply bridged structure for $\text{Cu}_2(\text{CO})_6$, but the trial geometries collapse to the dibridged structure **6c**. We also investigated a quadruply bridged $\text{Cu}_2(\text{CO})_6$ structure (D_{4h}), but no BP86 or BLYP stationary point geometry was found. With the BHLYP and B3LYP methods, such a stationary point has two or four imaginary vibrational frequencies, a very long Cu—Cu distance, and quite a high energy.

II. $\text{Cu}_2(\text{CO})_5$. The structure of $\text{Cu}_2(\text{CO})_5$ with the lowest energy (**5a**) is presented in Figure 2. It is a relatively unsymmetrical unbridged structure with C_s symmetry consisting of a $\text{Cu}(\text{CO})_3$ unit bonded to a $\text{Cu}(\text{CO})_2$ unit, and the analogy with the classical ethyl radical is clear. This structure is a genuine minimum, with no imaginary vibrational frequencies. With the BHLYP, B3LYP, BP86, and BLYP methods, $R(\text{Cu}-\text{Cu}) = 2.513, 2.528, 2.499,$ and 2.553 Å, respectively. These distances are shorter by 0.08, 0.10, 0.10, and 0.12 Å than those at the same levels of theory for the unbridged D_{3d} $\text{Cu}_2(\text{CO})_6$ structure **6b**. The shorter Cu—Cu distance in **5a** relative to **6b** could arise from an ionic component in the Cu—Cu bond of **5a**, arising from the nonequivalent nature of the $\text{Cu}(\text{CO})_3$ and $\text{Cu}(\text{CO})_2$ groups. There is another C_s unbridged stationary point **5b**, which differs from **5a** by only internal rotation. Note, however, that rotation barriers about metal—metal bonds can be small. Structure **5b** lies energetically above **5a** by only 0.1 or 0.2 kcal/mol (Table 2). There is a tiny imaginary vibrational frequency ($<20i$ cm^{-1}) for **5b**, which leads to the global minimum **5a**.

The monobridged structure **5c**, with C_{2v} symmetry, is analogous to the nonclassical bridging ethyl radical. The Cu—Cu bond distance (2.477, 2.489, 2.463, or 2.505 Å) shrinks from the unbridged structure **5a** by 0.04–0.05 Å. The C_{2v} structure **5c** is higher in energy than the C_s structure **5a**, and it has two or three imaginary vibrational frequencies depending on the computational method. Actually, structure **5c** is more like a loose complex composed of $\text{Cu}_2(\text{CO})_4$ and a carbonyl. We also found a doubly bridged C_{2v} structure **5d** with a higher energy. The Cu—Cu distance is significantly longer by 0.73–0.93 Å than that for structure **5a**; however, it is nearly equal to that predicted for the dibridged $\text{Cu}_2(\text{CO})_6$ structure **6c**. The doubly bridged structure **5d** is not a minimum, and it has three imaginary vibrational frequencies. The triply bridged D_{3h} structure **5e** is displayed in Figure 2. Depending on the computational method, the Cu—Cu distance is 3.193, 2.974, 2.789, or 2.853 Å, respectively. This structure is also high lying energetically, and has several imaginary vibrational frequencies.

III. $\text{Cu}_2(\text{CO})_4$. Figure 3 reveals our optimized structures for $\text{Cu}_2(\text{CO})_4$. Structure **4a** (C_s) is the global minimum, and structures **4b** (D_{2d}) and **4c** (D_{2h}) are energetically low-lying genuine minima. Structure **4a** can be viewed as an 18-electron $\text{Cu}(\text{CO})_3$ unit similar to half of $\text{Cu}_2(\text{CO})_6$ joined by a Cu—Cu bond to a 14-electron linear CuCO unit. Continuing our comparison with hydrocarbons, structure **4a** may be viewed as analogous to methylcarbene. The predicted Cu—Cu bond distance for **4a** of 2.425 Å (BHLYP), 2.412 Å (B3LYP), 2.382 Å (BP86) or 2.419 Å (BLYP) is shorter than that in the unbridged C_s structure for $\text{Cu}_2(\text{CO})_5$ **5a** by about 0.1 Å. The

Table 3. The Relative Energies of the $\text{Cu}_2(\text{CO})_4$ Structures, in kcal/mol

		BHLYP	B3LYP	BP86	BLYP
methyl carbene-like	4a	0.0	0.0	0.0	0.0
ethylene-like (twisted)	4b	5.9	3.8	3.5	2.9
ethylene-like	4c	6.8	4.8	5.4	4.6
dibridged	4d	33.7	27.5	9.1	13.4
tribridged	4e	29.3	25.8	21.0	22.4
tetrabridged	4f	69.2	88.5		

ethylene-like structures **4b** and **4c** are also unbridged, and lie higher in energy than **4a** by 2.9–5.9 kcal/mol and 4.6–6.8 kcal/mol, respectively. Structures **4b** and **4c** are different from each other by internal rotation. The D_{2d} structure **4b** lies slightly lower in energy (<2 kcal/mol) than the D_{2h} structure **4c**.

The dibridged C_{2h} (or D_{2h} by BLYP) structure **4d** for $\text{Cu}_2(\text{CO})_4$ may also be viewed as a genuine minimum (or very close to a true minimum), since there is a tiny imaginary vibrational frequency ($\sim 20i \text{ cm}^{-1}$) with the BHLYP and B3LYP methods and there are all real frequencies with the BP86 and BLYP methods. The BLYP method predicts a linear terminal Cu–C–O, and makes a D_{2h} structure, but the others methods predict a C_{2h} structure. This dibridged structure **4d** lies energetically above **4a** by 33.7 (BHLYP), 27.5 (B3LYP), 9.1 (BP86), or 13.4 (BLYP) kcal/mol. The copper–copper distance for this structure varies widely among the different methods, being 3.351 (BHLYP), 3.125 (B3LYP), 2.286 (BP86), or 2.319 (BLYP) Å. There is also a triply bridged structure with C_s (or C_{3v} by BHLYP) group point symmetry **4e**. Structure **4e** is more stable energetically than structure **4d** with the BHLYP and B3LYP methods, and displays all real vibrational frequencies (BHLYP) or one very small imaginary vibrational frequency (<20 $i \text{ cm}^{-1}$). The copper–copper bond length of this structure (**4e**) is shorter than the analogous triply bridged structure (**5e**) of $\text{Cu}_2(\text{CO})_5$. The BHLYP method predicts a linear terminal carbonyl arrangement for **4e**, and the structure has C_{3v} symmetry; but the other methods predict a bent ($162^\circ - 166^\circ$) terminal Cu–C–O, and the latter structure has C_s symmetry. The last structure studied for $\text{Cu}_2(\text{CO})_4$ is a quadruply bridged structure **4f** with D_{4h} symmetry. It is the least stable structure with very high energy (69–89 kcal/mol higher than **4a**, Table 3). The Cu–Cu separation is 4.133 Å (BHLYP) or 3.998 Å (B3LYP), which is very close to that for the quadruply bridged $\text{Cu}_2(\text{CO})_6$ structure, but we were unable to optimize either the BP86 or BLYP structure.

IV. $\text{Cu}_2(\text{CO})_3$. We obtained two unbridged structures with C_{3v} and C_s symmetry for $\text{Cu}_2(\text{CO})_3$, and these are structures **3a** and **3b** in Figure 4. Both structures are genuine minima and low lying in energy. The energy of the methyl carbyne-like structure **3a** is somewhat lower than that of the classical vinyl-like **3b** by 7.4 kcal/mol (BHLYP), 4.5 kcal/mol (B3LYP), 1.9 kcal/mol (BP86), or 1.2 kcal/mol (BLYP). The Cu–Cu bond distance (2.414, 2.398, 2.360, or 2.402 Å) for structure **3a** is longer than that for structure **3b** by 0.01–0.02 Å using the four DFT methods.

The monobridged vinyl-like structure **3c** and the dibridged structure **3d** both exhibit C_{2v} symmetry. Both are high lying energetically for $\text{Cu}_2(\text{CO})_3$, and have one or two imaginary vibrational frequencies. The copper–copper distances in structures **3c** and **3d** are longer than that for structure **3a** by about 0.3–0.7 Å. A triply bridged $\text{Cu}_2(\text{CO})_3$ structure **3e** with D_{3h} symmetry was also investigated in this study. The Cu–Cu distance of **3e** is significantly shorter than that for the monobridged and dibridged structures **3c** and **3d**, but somewhat longer than that for the unbridged structures **3a** and **3b**. Structure **3e**

Table 4. The Relative Energies of the $\text{Cu}_2(\text{CO})_3$ Structures, in kcal/mol

		BHLYP	B3LYP	BP86	BLYP
methyl carbyne-like	3a	0.0	0.0	0.0	0.0
classical vinyl radical-like	3b	7.4	4.5	1.9	1.2
bridging vinyl radical-like	3c	33.0	23.4	16.3	15.9
dibridged	3d	31.1	23.0	15.9	16.1
tribridged	3e	28.8	23.1	15.6	18.5

Table 5. The Relative Energies of the $\text{Cu}_2(\text{CO})_2$ Structures, in kcal/mol

		BHLYP	B3LYP	BP86	BLYP
vinylidene-like	2a	0.0	0.0	0.0	0.0
acetylene-like	2b	1.4	0.9	0.1	–0.6
<i>cis</i> bent acetylene-like	2c	1.4	0.4	–1.0	–1.5
<i>trans</i> bent acetylene-like	2d	1.3	0.3	–1.2	–1.7
dibridged	2e	25.7	18.8	12.2	14.0

lies close in energy to the two bridged structures and higher (by 16–29 kcal/mol) than the unbridged structures. The triply bridged structure **3e** has all real vibrational frequencies with the B3LYP, BP86, and BLYP methods, but this structure is a transition state with the BHLYP method.

V. $\text{Cu}_2(\text{CO})_2$. With the BHLYP and B3LYP methods the structure of $\text{Cu}_2(\text{CO})_2$ with the lowest energy is a vinylidene-like unbridged structure **2a** (Figure 5), with the two carbonyls on the same copper atom. But its energy is slightly higher than **2c** and **2d** as predicted by the BP86 and BLYP methods. The vinylidene-like structure is a genuine minimum. The Cu–Cu bond distance in this structure, namely, 2.373 Å (BHLYP), 2.355 Å (B3LYP), 2.321 Å (BP86), and 2.351 Å (BLYP), is about 0.4 Å shorter than that of our most favorable $\text{Cu}_2(\text{CO})_3$ structure **3a**.

Another unbridged linear $\text{Cu}_2(\text{CO})_2$ structure **2b** (analogous to acetylene) with constrained $D_{\infty h}$ symmetry was optimized in this research. It is not a minimum but has four small imaginary vibrational frequencies (π_g and π_u). Following the normal modes related to the imaginary vibrational frequencies, we were able to optimize the C_{2v} (*cis*) and C_{2h} (*trans*) unbridged structures **2c** and **2d**. Distortion from the linear structure **2b** to the bent structures **2c** and **2d** leads to a small energy lowering, with **2d** slightly more stable than **2c** (Table 5). They are both genuine minima, and their energies are close to that of **2a**. As a matter of fact, the energies of structures **2c** and **2d** are slightly higher than that of **2a** predicted by the BHLYP and B3LYP methods, but slightly lower by the BP86 and BLYP methods. The copper–copper bond distances for **2b**, **2c** and **2d** predicted by different methods are similar (Figure 5). For structure **2d** the Cu–Cu distances are 2.348 (BHLYP), 2.339 (B3LYP), 2.324 (BP86), and 2.342 (BLYP) Å, slightly shorter than that of **2a**. They are also somewhat shorter than that for the C_s $\text{Cu}_2(\text{CO})_3$ structure **3b**, by ~ 0.04 Å.

The only bridged structure found for $\text{Cu}_2(\text{CO})_2$ is the dibridged structure **2e**, with D_{2h} symmetry. Although it is a genuine minimum, its energy is much higher than other structures of $\text{Cu}_2(\text{CO})_2$ (Table 5). The dibridged structure also has a longer Cu–Cu bond distance (i.e., 2.998 Å BHLYP, 2.837 Å B3LYP, 2.707 Å BP86, and 2.774 Å BLYP) than the unbridged structures.

VI. $\text{Cu}_2(\text{CO})$. In 1977 Moskovits and Hulse³⁸ suggested four structures for $\text{Cu}_2(\text{CO})$ from the IR spectra. One of their structures is the linear Cu–Cu–C–O, two structures have bridging carbonyl groups (symmetric and asymmetric), and the last one has the structure Cu–C–O–Cu. When starting with

(38) Moskovits, M.; Hulse, J. E. *J. Phys. Chem.* **1977**, *81*, 2004.

Table 6. The Relative Energies of the Cu₂(CO) Structures, in kcal/mol

		BHLYP	B3LYP	BP86	BLYP
linear	1a	0.0	0.0	0.0	0.0
bridging	1b	33.9	28.0	25.3	25.1

the suggesting bridged geometries, we obtained three carbonyl structures. The linear structure **1a** and the symmetric bridged structure **1b** are shown in Figure 6. We did not locate the asymmetric bridged structure, and the cis bent structure Cu—C—O—Cu predicted by the BHLYP and B3LYP methods will not be discussed in this paper, since it does not correspond to any remotely conventional structure for the transition metal carbonyls.

The linear C_{∞v} structure **1a**, in which a terminal CO is bonded to a copper dimer, is a genuine minimum. The Cu—Cu bond distance (2.257–2.320 Å) in **1a** is the shortest among those predicted in this research. Results for the higher energy singly bridged Cu₂(CO) structure are found in the Supporting Information.

VII. Brief Summary. In the present study, we have discovered some interesting geometrical characteristics for the Cu₂(CO)_n systems. First, the global minima and the energetically low-lying structures for the Cu₂(CO)_n systems are all unbridged structures, and the bridged structures all have substantially higher energies. This is different from the other transition metal carbonyls, such as Fe₂(CO)_n, Co₂(CO)_n, and Ni₂(CO)_n,^{14–16} among which there are many bridged global minima or low-lying structures.

Second, the unbridged Cu₂(CO)_n systems may be viewed as two bonded fragments. Since the geometrical parameters of these fragments show small changes from the isolated radicals, they are almost transferable among the different structures. For example, the geometric parameters of Cu(CO)₃ fragments in **6a** (or **6b**) are very similar to those in the structure **5a** (or **5b**), **4a**, and **3a** (Figures 1–4). The Cu(CO)₃ radical has an unpaired electron on the 4*p* orbital of the Cu atom, so it has been called as “an inorganic isolobal analogue of methyl”.²³ However, its dimer Cu₂(CO)₆ (**6a** or **6b**) has a much smaller Cu—Cu—C angle (close to 90°) than the C—C—H angle in its “isolobal analogue” C₂H₆. The CH₃ radical in ethane has *sp*³ hybridization, but in Cu₂(CO)₆ the σ bond is formed by the interaction of the two singly occupied 4*p* orbitals from each Cu(CO)₃ unit, so that the Cu—Cu—C angle is close to 90°. Similarly the geometric parameters of the Cu(CO)₂ fragments are also almost transferable among the structures **5a** (or **5b**), **4b** (or **4c**), **3b**, and **2a** (Figures 2–5).

The Cu—Cu distance decreases among the Cu₂(CO)_n systems as the number of carbonyls decreases. For example, the B3LYP Cu—Cu distance decreases from 2.619 Å in **6a**, to 2.528 Å in **5a**, to 2.412 Å in **4a**, and to 2.398 Å in **3a** (Table 7), indicating stronger bonding in the structures with less carbonyls, from the perspective of a bond distance/bond energy correlation. Nevertheless, since the internal rotation barriers are so small for these unbridged structures, the Cu—Cu bonds should probably not be viewed as multiple bonds.

Another striking characteristic of the Cu₂(CO)_n systems is that most of the terminal carbonyls in Cu₂(CO)_n are bent, while in other transition-metal carbonyls (M=Cr, Mn, Fe, Co, and Ni) the terminal Cu—C—O angles are essentially linear.^{14–16} A qualitative explanation could be that the half-filled 4*s* orbital of the Cu atom and the 5*σ* orbital of CO cause significant repulsion, and this repulsion is decreased by the Cu—C—O bending.³⁹ Also, back-donation from the copper 3*d* orbitals into

Table 7. Copper—Copper Bond Lengths (in Å) of All of the Structures of Cu₂(CO)_x (x = 1–6)

<i>n</i>	no. of bridges	figure no. in text	BHLYP	B3LYP	BP86	BLYP
1	0	1a	2.320	2.291	2.257	2.279
	1	1b	3.465	3.343	3.204	3.273
2	0	2a	2.373	2.355	2.321	2.351
	0	2b	2.349	2.340	2.327	2.342
	0	2c	2.349	2.340	2.327	2.344
	0	2d	2.348	2.339	2.324	2.342
	2	2e	2.998	2.837	2.707	2.774
3	0	3a	2.414	2.398	2.360	2.402
	0	3b	2.392	2.386	2.365	2.390
	1	3c	3.172	2.799	2.648	2.748
	2	3d	3.215	3.080	2.966	3.023
	3	3e	2.698	2.552	2.458	2.520
4	0	4a	2.425	2.412	2.382	2.419
	0	4b	2.437	2.439	2.408	2.445
	0	4c	2.478	2.494	2.474	2.511
	2	4d	3.351	3.125	2.286	2.319
	3	4e	3.017	2.832	2.712	2.766
	4	4f	4.133	3.998		
5	0	5a	2.513	2.528	2.499	2.553
	0	5b	2.510	2.527	2.499	2.551
	1	5c	2.477	2.489	2.463	2.505
	2	5d	3.444	3.341	3.236	3.284
	3	5e	3.193	2.974	2.789	2.853
6	0	6a	2.619	2.660	2.636	2.714
	0	6b	2.595	2.626	2.602	2.671
	2	6c	3.484	3.372	3.255	3.308
	2	6d	2.975	3.006	2.927	3.015
	0	6e	2.490	2.498	2.475	2.517

π*(CO) will be less important than for the earlier transition metals, due to the contraction of the metal 3*d* orbital with atomic number. Although the linear terminal Cu—C—O moiety is seen in structures **5d** and **3d**, these structures were constrained in the geometry optimizations. Actually, the largest imaginary vibrational frequencies for structures **5d** and **3d** are related to the Cu—C—O bending modes. Unfortunately, when following these modes, we could not find the doubly bridged minima, because these structures collapse to the unbridged structures **5a** and **3a**.

B. Thermochemistry. Since 1923 numerous experiments based on the transport properties of heated copper in a stream of CO have demonstrated that the chances of isolating stable homoleptic copper carbonyls at room temperature in gram quantities are slight.^{40–43} However, carbon monoxide does weakly chemisorb onto copper films, and the infrared CO stretching bands suggest bonding to discrete atoms on the surface.^{42,43} Moreover, matrix isolation experiments show that the Cu₂(CO)_x species are readily synthesized at very low temperatures.^{20–26}

Table 8 lists the dissociation energies for the successive removal of carbonyls from Cu₂(CO)₆. The available experimental binding energy for CO and copper dimer (>25 kcal/mol)⁴⁴ is closest to the BLYP result. The B3LYP and BP86 results are also in reasonable agreement, but the BHLYP method predicts a poor binding energy for Cu₂(CO). From refs 14–16, we appreciate that the B3LYP method predicts reasonable thermochemistry, so we will discuss the dissociation energy

(39) (a) Fournier, R. J. *Chem. Phys.* **1993**, *98*, 8041. (b) Fournier, R. J. *Chem. Phys.* **1995**, *102*, 5396.

(40) Bertrand, C. R. C. *R. Acad. Sci.* **1923**, *177*, 997.

(41) Mond, E.; Heberlein, C. J. *Chem. Soc.* **1924**, *125*, 1222.

(42) Eischens, R. P.; Pliskin, W. A.; Francis, S. A. *J. Chem. Phys.* **1954**, *22*, 1986.

(43) Pritchard, J.; Sims, M. L. *Trans. Faraday Soc.* **1970**, *66*, 427.

(44) Lian, L.; Akhtar, F.; Hackett, P. A.; Rayner, D. M. *Int. J. Chem. Kinet.* **1994**, *26*, 85.

Table 8. Dissociation Energies (kcal/mol) for the Successive Removal of Carbonyl Groups from $\text{Cu}_2(\text{CO})_x$ ($x = 1-6$)^a

	BHLYP	B3LYP	BP86	BLYP	expt ^b
$\text{Cu}_2(\text{CO})_6 \rightarrow \text{Cu}_2(\text{CO})_5 + \text{CO}$	14.8	18.9	24.6	21.2	
$\text{Cu}_2(\text{CO})_5 \rightarrow \text{Cu}_2(\text{CO})_4 + \text{CO}$	9.2	15.7	22.3	18.6	
$\text{Cu}_2(\text{CO})_4 \rightarrow \text{Cu}_2(\text{CO})_3 + \text{CO}$	7.4	15.3	25.3	21.1	
$\text{Cu}_2(\text{CO})_3 \rightarrow \text{Cu}_2(\text{CO})_2 + \text{CO}$	14.1	18.5	24.6	20.2	
$\text{Cu}_2(\text{CO})_2 \rightarrow \text{Cu}_2(\text{CO}) + \text{CO}$	9.6	15.2	21.5	17.7	
$\text{Cu}_2(\text{CO}) \rightarrow \text{Cu}_2 + \text{CO}$	12.2	20.3	31.2	27.6	>25

^a All of the results reported here refer to the lowest energy structures of $\text{Cu}_2(\text{CO})_x$, i.e., **6a**, **5a**, **4a**, **3a**, **2a**, and **1a**. ^b Ref 43.

mainly based on the B3LYP results. It is clear that the dissociation energies for $\text{Cu}_2(\text{CO})_n$ systems are much smaller than those of $\text{Fe}_2(\text{CO})_n$ and $\text{Co}_2(\text{CO})_n$.^{15,16} Thus the binuclear homoleptic copper carbonyls are less stable than the iron and cobalt carbonyls. The general consensus of opinion suggests that the lower stability of copper carbonyls is a reflection of the stability of a full 3d valence shell and a situation not conducive to $d_{\pi}(\text{Cu}) \rightarrow \pi^*(\text{CO})$ bonding.⁴⁵

Table 8 shows that $\text{Cu}_2(\text{CO})_6$ (**6a**), $\text{Cu}_2(\text{CO})_3$ (**3a**), and $\text{Cu}_2(\text{CO})$ (**1a**) may be somewhat more stable than the other binuclear copper carbonyls, since the values of the B3LYP dissociation energies for these systems are slightly larger than the others. Thus, we suspect that these compounds should be more readily detected by infrared and UV–vis spectroscopy. In this connection the experimental CO stretching frequencies of $\text{Cu}_2(\text{CO})_6$ and $\text{Cu}_2(\text{CO})$ have been obtained at cryogenic temperatures. Huber et al.,²⁰ and Chenier et al.,²⁵ have reported IR absorptions for $\text{Cu}_2(\text{CO})_6$, while Moskovits and Hulse³⁷ obtained a $\nu(\text{CO})$ frequency for the $\text{Cu}_2(\text{CO})$ system.

Even for the “saturated” $\text{Cu}_2(\text{CO})_6$, synthesis by conventional techniques does not appear to be feasible. From the extremely low experimental value of the $\sigma \rightarrow \sigma^*$ transition energy of $\text{Cu}_2(\text{CO})_6$ (417 nm)^{20,46} compared to the $\sigma \rightarrow \sigma^*$ energies of other M–M bonded carbonyls (300 to 350 nm)^{47,48} that are stable at ambient temperature, one is led to the conclusion that the Cu–Cu bond dissociation energy in $\text{Cu}_2(\text{CO})_6$ is low.

C. Vibrational Frequencies. Harmonic vibrational frequencies have been evaluated for all structures described above. Our discussion turns to the question of whether the geometries optimized are in fact genuine minima, and the imaginary vibrational frequencies for all the structures are listed in Table 9. As discussed elsewhere^{15,16} the use of numerical integration schemes in all current DFT methods means that total energies are rarely accurate to better than 0.0001 hartree. Similarly, small vibrational frequencies can be off by 50i cm^{-1} , bringing into question in some cases whether a stationary point is a genuine minimum or a transition state. When one reports imaginary vibrational frequencies smaller in magnitude than 50 cm^{-1} , caution in interpretation is advised.

With respect to the $\text{Cu}_2(\text{CO})_6$ vibrational frequencies, the unbridged structures **6a** and **6b** with D_{3h} and D_{3d} symmetry and the D_{2h} dibridged structure **6c** are considered to be genuine minima, although for **6a**, there is a very tiny imaginary frequency predicted by the BP86 and BLYP methods (Table 9). Since the unbridged structures **6a** and **6b** are the lowest in energy, we conclude that these structures are the most stable geometries for $\text{Cu}_2(\text{CO})_6$. Chenier et al.²⁵ found two IR

absorptions for $\text{Cu}_2(\text{CO})_6$ in adamantane (2014 and 2035 cm^{-1}) and one in cyclohexane (2035 cm^{-1}). Huber et al.²⁰ have reported that there are two absorptions for the $\text{Cu}_2(\text{CO})_6$ complex (2039 and 2003 cm^{-1}) in argon at 10–15 K. They are in good agreement from our B3LYP results: 2068 (a'') and 2099 (e') cm^{-1} for the structure **6a**, or 2068 (a'') and 2090 (e') cm^{-1} for the structure **6b**, which are predicted to have large infrared intensities. Huber also inferred that $\text{Cu}_2(\text{CO})_6$ has a D_3 rotary configuration rather than the more highly symmetrical D_{3h} or D_{3d} configurations. It might appear that there is a contradiction between Huber's results and ours. However, since there is very small potential barrier (<0.5 kcal/mol predicted by the B3LYP method) between the D_{3h} and D_{3d} structures, it is easy to rotate around the copper–copper σ bond. Therefore, it is reasonable for the experimentalists to observe an intermediate configuration. The C_{2v} structure **6e** has a substantial imaginary frequency (b_1 mode) above 100i cm^{-1} with all the four methods, i.e., 130i (BHLYP), 174i (B3LYP), 186i (BP86), and 180i cm^{-1} (BLYP), which would lead to structure **6b**.

For $\text{Cu}_2(\text{CO})_5$ the lowest energy unbridged structure **5a** has no imaginary vibrational frequency, and it is the global minimum. The other unbridged structure **5b** has one very small imaginary frequency at 16i (BHLYP), 8i (B3LYP), 6i (BP86), and 7i cm^{-1} (BLYP), which leads to **5a**. There are two or three imaginary vibrational frequencies for the higher energy mono-bridged C_{2v} structure **5c**, which collapses to **5b**. The dibridged structure **5d** has several substantial imaginary vibrational frequencies, and it is a third-order stationary point. Following one of the modes related to the imaginary vibrational frequencies, **5d** will go to either structure **5a** or structure **5b**.

For $\text{Cu}_2(\text{CO})_4$ the unbridged structures **4a**, **4b**, and **4c** have all real vibrational frequencies, indicating genuine minima. The quadruply bridged D_{4h} structure **4f** is also a genuine minimum, but with high energy. The dibridged and tribridged structures **4d** and **4e** with higher energies appear to be genuine minima or very close to minima, because each has at most a tiny imaginary vibrational frequency. For the dibridged structure **4d** an imaginary frequency is predicted by the BHLYP (15i cm^{-1}) and B3LYP (22i cm^{-1}) methods, and for **4e** such is predicted by the B3LYP (14i cm^{-1}), BP86, (20i cm^{-1}), or BLYP (15i cm^{-1}) methods.

For $\text{Cu}_2(\text{CO})_3$, the two unbridged C_{3v} and C_s structures (**3a** and **3b**) are obviously genuine minima. For the mono-bridged structure **3c**, there is one imaginary vibrational frequency (b_1 mode), namely 36i cm^{-1} (BHLYP), 87i cm^{-1} (B3LYP) 69i cm^{-1} (BP86), or 46i cm^{-1} (BLYP). Following this mode will lead to structure **3b**. The dibridged C_{2v} structure **3d**, with a longer copper–copper bond, appears not to be a genuine minimum with larger imaginary frequencies 57i cm^{-1} (BHLYP), 155i, 16i cm^{-1} (B3LYP), 231i, 22i cm^{-1} (BP86), or 231i, 31i cm^{-1} (BLYP). Following the normal mode related to the largest imaginary frequency will lead to the global minimum **3a**. The triply bridged D_{3h} structure **3e** is a minimum predicted by three DFT methods except for the BHLYP method, which predicts one (120i cm^{-1}) imaginary vibrational frequency.

Clearly, all the structures of $\text{Cu}_2(\text{CO})_2$ are genuine minima except for the linear structure **2b**. Structure **2b** has four imaginary vibrational frequencies (two pairs of degenerate modes π_g and π_u), and it will collapse to either **2c** or **2d** as a minimum.

In their study of interactions of CO with very small copper clusters Moskovits and Hulse³⁸ concluded that the absorptions at 2116 and 1871 cm^{-1} in the IR spectrum belong to species of stoichiometry Cu_2CO . The fundamental at 2116 cm^{-1} may arise

(45) Cotton, F. A.; Marks, T. J. *J. Am. Chem. Soc.* **1970**, *92*, 5114.

(46) Levenson, R. A.; Gray, H. B.; Ceasar, G. P. *J. Am. Chem. Soc.* **1970**, *92*, 3653.

(47) Fawcett, J. P.; Poë, J. A.; Twigg, M. V.; *J. Chem. Soc., Chem. Commun.* **1973**, 267.

(48) Wrighton M.; Bredezen, D. *J. Organomet. Chem.* **1973**, *50*, C35.

Table 9. Imaginary Vibrational Frequencies for All of the Structures of $\text{Cu}_2(\text{CO})_x$ ($x = 1-6$)

			BHLYP	B3LYP	BP86	BLYP
$\text{Cu}_2(\text{CO})_6$	6a	D_{3h}	none	none	11i	8i
	6b	D_{3d}	none	none	none	none
	6c	D_{2h}	none	none	none	none
	6d	D_{2h}	none	none	none	none
	6e	C_{2v}	130i, 4i	174i	186i, 35i	180i
$\text{Cu}_2(\text{CO})_5$	5a	C_s	none	none	none	none
	5b	C_s	16i	8i	6i	7i
	5c	C_{2v}	84i, 28i	94i, 26i	177i, 99i, 25i	109i, 48i
	5d	C_{2v}	146i, 78i, 9i	289i, 161i, 12i	422i, 214i, 16i	446i, 253i, 13i
	5e	C_{2v}	none	none	none	none
$\text{Cu}_2(\text{CO})_4$	4a	C_s	none	none	none	none
	4b	D_{2d}	none	none	none	none
	4c	D_{2h}	none	none	none	none
	4d	$C_{2h}(D_{2h})$	15i	22i	none	none
	4e	$C_s(C_{3v})$	none	14i	20i	15i
$\text{Cu}_2(\text{CO})_3$	4f	D_{4h}	none	none	-	-
	3a	C_{3v}	none	none	none	none
	3b	C_s	5i	none	none	none
	3c	C_{2v}	36i	87i	69i	46i
	3d	C_{2v}	57i	155i, 16i	231i, 22i	231i, 31i
$\text{Cu}_2(\text{CO})_2$	3e	D_{3h}	120i	none	none	none
	2a	C_{2v}	none	none	none	none
	2b	$D_{\infty h}$	25i, 13i	56i, 32i	67i, 39i	69i, 41i
	2c	C_{2v}	10i	none	none	none
	2d	C_{2h}	10i	none	none	none
$\text{Cu}_2(\text{CO})$	2e	D_{2h}	none	none	none	none
	1a	$C_{\infty v}$	none	none	none	none
	1b	C_{2v}	none	none	none	none

from a terminal CO, while the lower frequency could belong to a bridging CO. In our study, the unbridged structure **1a** with low-lying energy (Table 6) is a CO terminally bonded species. The $\nu(\text{CO})$ vibrational frequency is predicted to be 2327 cm^{-1} (BHLYP), 2174 cm^{-1} (B3LYP), 2063 cm^{-1} (BP86), or 2046 cm^{-1} (BLYP). The results are close to the experimental IR value. The monobridged C_{2v} structure **1b** is also a minimum. As far as the $\nu(\text{CO})$ vibrational frequency is concerned (i.e., 1874 cm^{-1} BHLYP, 1814 cm^{-1} B3LYP, 1751 cm^{-1} BP86, or 1740 cm^{-1} BLYP), we conclude that the experimental IR $\nu(\text{CO})$ of 1871 cm^{-1} is in agreement with the theoretical results for the monobridged structure **1b**. It further confirms that structure **1b** is a stable species.

Discussion

Our previous computational studies on unsaturated homoleptic binuclear carbonyls of iron,¹⁵ cobalt,¹⁶ and nickel,¹⁴ i.e., those with fewer carbonyl groups than $\text{Fe}_2(\text{CO})_9$, $\text{Co}_2(\text{CO})_8$, and $\text{Ni}_2(\text{CO})_7$, respectively, indicate that in most cases the lowest energy isomers have structures with metal–metal multiple bonds and 18-electron configurations for the transition metal atoms. The one exception is $\text{Co}_2(\text{CO})_7$, in which the lowest energy structure has an 18-electron five-coordinate $[\text{Co}]\text{Co}(\text{CO})_4$ fragment joined by a Co–Co single bond to a 16-electron square planar $[\text{Co}]\text{Co}(\text{CO})_3$ fragment without any bridging carbonyl groups (Figure 7a). In this discussion the abbreviations $[\text{Co}]$ and $[\text{Cu}]$ refer to a metal–metal bond of the unbracketed central metal atom to the bracketed metal atom where the brackets refer to ligands around the bracketed metal atom that are irrelevant to the local environment of the unbracketed metal atom.

A situation similar to that for $\text{Co}_2(\text{CO})_7$ occurs in most of the lowest energy binuclear copper carbonyl structures discussed in this paper. The basic building blocks for the binuclear copper carbonyls are the 18-electron tetrahedral $[\text{Cu}]\text{Cu}(\text{CO})_3$ fragment, the 16-electron trigonal planar $[\text{Cu}]\text{Cu}(\text{CO})_2$ fragment, and the 14-electron linear $[\text{Cu}]\text{Cu}(\text{CO})$ fragment (Figure 7b), as well as the bare copper atom. The structures of all of the lowest energy isomers of the binuclear copper carbonyls found in this

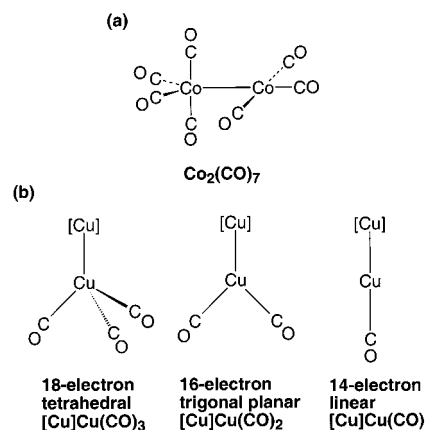


Figure 7. (a) Optimized structure of $\text{Co}_2(\text{CO})_7$ predicted in ref 16. (b) The 18-electron tetrahedral $[\text{Cu}]\text{Cu}(\text{CO})_3$ unit, the 16-electron trigonal planar $[\text{Cu}]\text{Cu}(\text{CO})_2$ unit, and the 14-electron linear $[\text{Cu}]\text{Cu}(\text{CO})$ unit.

work may be constructed by joining a suitably chosen pair of these building blocks with a Cu–Cu single bond. Thus the lowest energy structures for $\text{Cu}_2(\text{CO})_6$, namely structures **6a** and **6b**, arise from joining two tetrahedral $[\text{Cu}]\text{Cu}(\text{CO})_3$ fragments. Similarly structure **5a** for $\text{Cu}_2(\text{CO})_5$ arises from joining a tetrahedral $[\text{Cu}]\text{Cu}(\text{CO})_3$ fragment to a trigonal $[\text{Cu}]\text{Cu}(\text{CO})_2$ fragment. This structure is somewhat analogous to that found¹⁶ for $\text{Co}_2(\text{CO})_7$, but with one less carbonyl group on each metal atom. The two lowest lying structures for $\text{Cu}_2(\text{CO})_4$ correspond to two linked trigonal planar $[\text{Cu}]\text{Cu}(\text{CO})_2$ fragments (**4b**) and a tetrahedral $[\text{Cu}]\text{Cu}(\text{CO})_3$ fragment linked to a linear $[\text{Cu}]\text{Cu}(\text{CO})$ fragment (**4a**). Similarly the two lowest lying structures for $\text{Cu}_2(\text{CO})_3$ correspond to a tetrahedral $[\text{Cu}]\text{Cu}(\text{CO})_3$ unit bonded to a bare copper atom (**3a**) and a trigonal planar $[\text{Cu}]\text{Cu}(\text{CO})_2$ unit bonded to a linear $[\text{Cu}]\text{Cu}(\text{CO})$ unit (**3b**). The lowest energy $\text{Cu}_2(\text{CO})_2$ structures are derived from linear $[\text{Cu}]\text{Cu}(\text{CO})$ fragments with relatively minor distortions, whereas the lowest energy $\text{Cu}_2(\text{CO})$ structure is simply a linear $[\text{Cu}]\text{Cu}(\text{CO})$ fragment with one bare copper atom.

The tendency of copper, as well as its heavier congeners silver and gold, to form stable 16-electron planar complexes and 14-electron linear complexes has been recognized for more than 50 years. As early as 1961 Nyholm⁴⁹ noted the possibility of shifting of one or two of the outer *p* orbitals in coinage metals (silver, copper, and gold) to such high energies that they no longer participate in the chemical bonding and the accessible *spd* manifold is no longer spherical (isotropic). If one *p* orbital is so shifted to become antibonding, then the accessible *spd* valence orbital manifold contains only eight orbitals (sp^2d^5) corresponding to a 16-electron configuration for the central metal atom and trigonal or square planar coordination, depending upon the number of ligands available.⁵⁰ If two *p* orbitals are shifted to antibonding energy levels, then the accessible *spd* valence orbital manifold contains only seven orbitals (spd^5) corresponding to a 14-electron configuration for the central metal atom. In this case the central metal atom is two-coordinate with linear coordination of the two ligands.

The reluctance for pairs of copper atoms to form multiple bonds in unsaturated binuclear copper carbonyls may relate to

the difficulty of breaching the filled d^{10} shell of a neutral copper atom. This may be related to the pseudohalogenic nature of copper and its heavier congeners. In the case of copper the diamagnetic Cu_2 dimer with a single Cu–Cu σ bond similar to the halogens X_2 is a stable gas-phase species.⁵¹ The heavier congeners of copper, namely silver and gold, even form the stable anions Ag^- (ref 51) and Au^- (refs 53 and 54) under suitable conditions. Thus structures **3a** for $Cu_2(CO)_3$, **2a** for $Cu_2(CO)_2$, and **1a** for $Cu_2(CO)$ may be considered to be analogous to hypothetical 18-electron tetrahedral carbonyl halides $Cu(CO)_3X$, 16-electron trigonal planar carbonyl halides $Cu(CO)_2X$, and 14-electron linear carbonyl halides, $Cu(CO)X$, respectively.

Acknowledgment. This research was supported by the National Key Laboratory of Theoretical and Computational Chemistry of Jilin University in China, and the US National Science Foundation, Grant CHE-98153897.

IC010769S

(49) Nyholm, R. S. *Proc. Chem. Soc.* **1961**, 273.

(50) King, R. B. *J. Chem. Inf. Comput. Sci.* **1994**, 34, 410.

(51) Morse, M. D. *Chem. Rev.* **1986**, 86, 1066–1069 and references therein.

(52) Tran, N. E.; Lagowski, J. J. *Inorg. Chem.* **2001**, 40, 1067.

(53) Sommer, A. H. *Nature* **1943**, 152, 215.

(54) Grosch, G. H.; Range, K.-J. *J. Alloys Compounds* **1996**, 233, 30